Association of *CXCR6* with COVID-19 severity: Delineating the host genetic factors in transcriptomic regulation

Yulin Dai[1†], Junke Wang[2†], Hyun-Hwan Jeong[1], Wenhao Chen[3,4], Peilin Jia[1], Zhongming Zhao[1,2,5*]

[1]Center for Precision Health, School of Biomedical Informatics, The University of Texas Health Science Center at Houston, Houston, TX 77030, USA

[2]MD Anderson Cancer Center UTHealth Graduate School of Biomedical Sciences, Houston, TX, USA

[3]Immunobiology and Transplant Science Center, Department of Surgery, Houston Methodist Research Institute and Institute for Academic Medicine, Houston Methodist Hospital, Houston, TX 77030, USA

[4]Department of Surgery, Weill Cornell Medicine, Cornell University, New York, NY 10065, USA

[5]Human Genetics Center, School of Public Health, The University of Texas Health Science Center at Houston, Houston, TX 77030, USA

[†] Contribute equally to this work.

[*] To whom correspondence should be addressed:
Zhongming Zhao, Ph.D.
Center for Precision Health
School of Biomedical Informatics
The University of Texas Health Science Center at Houston
7000 Fannin St. Suite 600 Houston, TX 77030
Phone: 713-500-3631
Email: Zhongming.Zhao@uth.tmc.edu

Abstract

Background: The coronavirus disease 2019 (COVID-19) is an infectious disease that mainly affects the host respiratory system with ~80% asymptomatic or mild cases and ~5% severe cases. Recent genome-wide association studies (GWAS) have identified several genetic loci associated with the severe COVID-19 symptoms. Delineating the genetic variants and genes is important for better understanding its biological mechanisms.

Methods: We implemented integrative approaches, including transcriptome-wide association studies (TWAS), colocalization analysis and functional element prediction analysis, to interpret the genetic risks using two independent GWAS datasets in lung and immune cells. To understand the context-specific molecular alteration, we further performed deep learning-based single cell transcriptomic analyses on a bronchoalveolar lavage fluid (BALF) dataset from moderate and severe COVID-19 patients.

Results: We discovered and replicated the genetically regulated expression of *CXCR6* and *CCR9* genes. These two genes have a protective effect on the lung and a risk effect on whole blood, respectively. The colocalization analysis of GWAS and *cis*-expression quantitative trait loci highlighted the regulatory effect on *CXCR6* expression in lung and immune cells. In the lung resident memory $CD8^+$ T (T_{RM}) cells, we found a 3.32-fold decrease of cell proportion and lower expression of *CXCR6* in the severe than moderate patients using the BALF transcriptomic dataset. Pro-inflammatory transcriptional programs were highlighted in T_{RM} cells trajectory from moderate to severe patients.

Conclusions: *CXCR6* from the *3p21.31* locus is associated with severe COVID-19. *CXCR6* tends to have a lower expression in lung T_{RM} cells of severe patients, which aligns with the protective effect of *CXCR6* from TWAS analysis. We illustrate one potential mechanism of host

genetic factor impacting the severity of COVID-19 through regulating the expression of *CXCR6* and T_{RM} cell proportion and stability. Our results shed light on potential therapeutic targets for severe COVID-19.

Keywords: Host genetics, COVID-19, TWAS, colocalization, single cell RNA sequencing, *CXCR6*, lung resident memory CD8$^+$ T (T_{RM}) cell

Background

The coronavirus disease 2019 (COVID-19) pandemic has already infected over 100 million people and caused numerous morbidities and over 2 million death worldwide as of January 2021. The virus is evolving fast with new variants being emerged in the world [1, 2]. A huge disparity in the severity of symptoms in different patients has been observed. In some of the patients, only mild symptoms or even no symptoms are shown and little treatment or interventions are required while a subset of patients experience rapid disease progression to respiratory failure and need urgent and intensive care [3]. Although age and sex are major risk factors of COVID-19 disease severity [4], it remains largely unclear about the factors leading to the variability on COVID-19 severity and which group of individuals confer intrinsic susceptibility to COVID-19.

Several genome-wide association studies (GWAS) have been carried out and one genomic risk locus, *3p21.31*, has been replicated to be associated with the critical illness. One recent study by the Severe COVID-19 GWAS Group identified *3p21.31* risk locus for the susceptibility to severe COVID-19 with respiratory failure [5]. This GWAS signal was then replicated in a separate meta-analysis comprising in total 2,972 cases from 9 cohorts by COVID-19 Host Genetics Initiative (HGI) round 4 alpha. However, there is a cluster of 6 genes

(*SLC6A20*, *LZTFL1*, *CCR9*, *FYCO1*, *CXCR6,* and *XCR1*) nearby the lead SNP rs35081325 within a complex linkage disequilibrium (LD) structure, which makes the "causal" gene and functional implication of this locus remain elusive [5, 6].

The majority of GWAS variants are located in non-coding loci, many of which are in the enhancer or promoter regions, playing roles as *cis*- or *trans*- regulatory elements to alter gene expression [7]. Although the function of non-coding variants could not be directly interrupted by their locations, their mediation effect on gene expression could be inferred by the expression quantitative trait loci (eQTL) analysis. In recent years, large consortia like GTEx (Genotype-Tissue Expression), eQTLGen Consortium, and DICE (database of immune cell expression) have generated rich eQTLs resources in diverse tissues and immune-related cell types [7-9]. A variety of statistical approaches such as transcriptome-wide association study (TWAS) analysis and colocalization analysis have successfully interpreted the target genes of non-coding variants by integrating the context-specific eQTLs [10-13].

Recent advances in single cell transcriptome sequencing provide unprecedented opportunities to understand the biological mechanism underlying disease pathogenesis at the single cell and cell type levels [14-16]. The recent generation of single cell RNA-sequencing (scRNA-seq) data from the bronchoalveolar lavage fluid (BALF) of moderate and severe COVID-19 patients has revealed the landscape of the gene expression changes in major immune cells. However, the transcriptome alteration in specific subpopulations remains mostly unexplored [17].

In this study, we aimed to connect the genetic factors with the context-specific molecular phenotype in COVID-19 patients. As illustrated in **Fig. 1**, we designed a multi-level workflow to dissect the genetically regulated expression (GReX) that contributed to severe COVID-19. We

performed TWAS and colocalization analyses with a broad collection of eQTL datasets at the tissue and cellular levels. We further integrated the BALF single cell transcriptome dataset to explore the cellular transcriptome alterations in severe and moderate COVID-19 patients. Lastly, we proposed a hypothetical mechanism, connecting our multi-layer evidence in host genetic factors, gene (*CXCR6*), and single cell transcriptome features with the severity of COVID-19.

Methods

GWAS dataset

We obtained GWAS summary statistics for the phenotype "severe COVID-19 patients vs population" (severe COVID-19) from two separate meta-analyses carried out by the COVID-19 Host Genetics Initiative (HGI, https://www.covid19hg.org/) and the Severe COVID-19 GWAS Group (SCGG) [5]. The $GWAS_{HGI}$ A2 round 4 (alpha) cohort consists of 12,816,037 SNPs from the association study of 2,972 very severe respiratory confirmed COVID-19 cases and 284,472 controls with unknown SARS-CoV-2 infection status from nine independent studies in a majority of the European Ancestry population. The $GWAS_{SCGG}$ dataset is from the first GWAS of severe COVID-19 [5], including 8,431,427 SNPs from the association study conducted from 1,980 COVID-19 confirmed patients with severe disease status and 2,205 control participants from two separate cohorts in Europe.

Transcriptome-wide association analysis

We performed TWAS analyses of severe COVID-19 using S-PrediXcan [18] to prioritize GWAS findings and identify eQTL-linked genes. S-PrediXcan is a systematic approach that integrates GWAS summary statistics with publicly available eQTL data to translate the evidence

of association with a phenotype from the SNP level to the gene level. Briefly, prediction models were built by a flexible and generic approach multivariate adaptive shrinkage in R package (MASHR) using variants with a high probability of being causal for QTL and tissue expression profiles from the GTEx version 8 [7, 19]. We chose three tissues that were relevant to SARS-CoV-2 infection, including lung, whole blood, and spleen. Then, we ran S-PrediXcan scripts (downloaded from https://github.com/hakyimlab/MetaXcan, accessed on 10/10/2020) with each of the three tissue-specific models in two severe COVID-19 GWAS datasets respectively. The threshold used in TWAS significance was adjusted by Bonferroni multiple test correction with the ~10,000 genes. We defined the strict significance as $p < 5 \times 10^{-6}$ ($|z| > 4.56$) and suggestive significance as $p < 5 \times 10^{-5}$ ($|z| > 4.06$).

Colocalization analysis

Colocalization was performed to validate significant TWAS associations using two recent and cutting-edge statistical analysis approaches: eCAVIAR [20] and fastENLOC [21], which aim to identify a single genetic variant that has shared causality between expression and GWAS trait. Both eCAVIAR and fastENLOC could assess the colocalization posterior probability (CLPP) for two traits at a locus, while eCAVIAR allows for multiple causal variants and fastENLOC features accountability for allelic heterogeneity in expression traits and high sensitivity of the methodology. We ran eCAVIAR between significant TWAS genes and GWAS trait with a maximum of five causal variants per locus and defined a locus as 50 SNPs up- and down- stream of the tested causal variant, following the recommendation in the original paper. The eCAVIAR was downloaded from https://github.com/fhormoz/caviar/ (accessed on 10/25/2020). The

biallelic variants from the 1,000 Genomes Project phase III in European ancestry were used as an LD reference [22]. We defined CLPP > 0.5 as having strong colocalization evidence.

To run fastENLOC, we first prepared probabilistic eQTL annotations to generate the cis-eQTL's posterior inclusion probability (PIP). Specifically, we applied the tissue-specific data from GTEx and T follicular cell-specific data from the DICE database [9] using the integrative genetic association analysis with the deterministic approximation of posteriors (DAP-G) package [23]. Then, GWAS summary statistics were split into approximately LD-independent regions defined by reference panel from European ancestry and z-scores were converted to PIP. We downloaded the fastENLOC from https://github.com/xqwen/fastenloc (accessed on 10/25/2020) and followed the guideline to yield regional colocalization probability (RCP) for each independent GWAS locus using each tissue- or cell type-specific eQTL annotation. We defined RCP > 0.5 as having strong colocalization evidence.

Functional genomics annotations

To better understand the potential function of the variants identified by GWAS analyses and how they mediate the regulatory effect, we annotated significant SNPs using publicly available data. We obtained the tissue and cellular level eQTL data from the following resources: 1) the eQTLGen consortium [24] eQTLs generated from 30,912 whole blood samples; 2) Biobank-based Integrative Omics Studies (BIOS) eQTLs generated from 2,116 healthy adults [25]; 3) The GTEx v8 [7] eQTLs of the lung, whole blood, and spleen tissues; 4) DICE database [9] with cellular eQTLs of 9 available T cell subpopulations. To identify the genomic annotation of the significant SNPs, we downloaded the multivariate hidden Markov model (ChromHMM) [26] processed chromatin-state data of 17 lung and T cell lines from the Roadmap Epigenomics

project [27]. To explore the potential chromatin looping of GWAS locus, we used publicly available chromatin interaction (Hi-C) data [28] at a resolution of 40Kb on IMR90, a normal lung fibroblast cell line. The Hi-C data has been used to identify specific baits and targets from distant chromatin regions that frequently interact with each other. Variants within the regulatory regions can be connected to the potential gene targets and thus mediate the gene expression. Statistical tests of bait-target pairs were conducted to define significant bait interaction regions and their targets. The eQTL associations and chromatin-state information and Hi-C interactions were processed and plotted using the R Bioconductor package gviz in R version 4.0.3 [29].

Differentially expressed gene analysis in resident memory CD8$^+$ T cells

We use the recently published scRNA-seq dataset of bronchoalveolar lavage fluids (BALF) samples from nine patients (three moderate and six severe) with COVID-19 [17, 30]. We adapted the original annotation [17] and followed their method to calculate the resident memory CD8$^+$ T (T_{RM}) cells signature score by using 31 markers (14 positive markers and 17 negative markers) for all annotated CD8$^+$ T cells [31, 32]. We excluded cells with CD4$^+$ expression and defined the top 50% scored cells as the T_{RM} cells. Lastly, we conducted a non-parametric Wilcoxon rank sum test by the function of "FindAllMarkers" from R package Seurat [33](version 3.1.5 in R version 3.5.2) to perform the differentially expressed genes (DEG) analysis between moderate and severe patients.

Cell trajectory and transcriptional program analysis in T_{RM} cells

We used the R package Slingshot [34] to infer cell transition and pseudotime from the scRNA-seq data. Specifically, we first used the expression data to generate the minimum spanning tree

of cells in a reduced-dimensionality space [t-Distributed Stochastic Neighbor Embedding (tSNE) project from top 30 principle components of top 3,000 variable genes] assuming there are two major clusters (moderate and severe T_{RM} cells). We then applied the principal curve algorithm [35] to infer an one-dimensional variable (pseudotime) representing the each cell's trajectory along the transcriptional progression. We used our in-house machine learning tool, DrivAER (Driving transcriptional programs based on AutoEncoder derived relevance scores) [36], to identify potential transcriptional programs (e.g., gene sets of pathways or transcription factors (TF)s) that potentially regulate the inferred cell trajectory between the moderate and severe patients. To avoid the potential noise from the low expression genes, we excluded those genes expressed in < 10% cells. DrivAER took gene-expression and pseudotime inferred from previous cell trajectory results (Slingshot) and calculated each gene's relevance score by performing cellular manifold by using Deep Count Autoencoder [37] and a random forest model with out-of-bag score calculation as the relevance score. The transcriptional program annotations were from the hallmark pathway gene sets from MSigDB [38] and transcription factor (TF) target gene sets from TRRUST [39]. To calculate the relevance score, we used the "calc_relevance" function with the following parameters: min_targets = 10, ae_type = "nb-conddisp", epoch=100, early_stop=3, and hidden_size = "(8,2,8)". The relevance score (R^2 coefficient of determination) indicates the proportion of variance in the pseudotime explained by target genes of transcription factor or genes in the hallmark pathways.

DNA motif recognition analysis of genome-wide significant SNPs

We used the function "variation-scan" of the online tool RSAT (http://rsat.sb-roscoff.fr/index.php, accessed on 01/15/2020) [40] to predict the binding effect of all the

significant SNPs at the *3p21.31* locus. We defined the TF with Bonferroni corrected $p < 0.05$ as the significant TF. Later, we compared them with the TF with high relevance score from the DrivAER analysis above. The position weight matrices (PWMs) for all the TFs were downloaded from cis-BP Database (http://cisbp.ccbr.utoronto.ca/) version 2019-06_v2.00) [41] and sequence logos representing motif binding sites were generated using R package seqLogo version 1.54.3 in R version 3.5.2.

Results

TWAS analysis identified and replicated two chemokine receptor genes

We utilized the latest S-PrediXcan MASHR models trained with GTEx v8 data for TWAS analyses in lung and whole blood on two GWAS datasets of susceptibility to severe COVID-19 [19]. In the HGI cohort, we found that a decreased expression of *CXCR6*, which encodes C-X-C chemokine receptor type 6, in the lung was associated with an increased risk for the development of severe COVID-19 symptoms ($p = 1.57 \times 10^{-17}$, $z = -8.53$), and this result was then replicated in the SCGG cohort ($p = 2.84 \times 10^{-5}$, $z = -4.19$, suggestive significant) (**Fig. 2** and **Table 1**). Likewise, an increased expression of *CCR9*, which encodes C-C chemokine receptor type 9, in whole blood was associated with an increased risk for the development of severe COVID-19 complications in $GWAS_{HGI}$ cohort ($p = 7.90 \times 10^{-11}$, $z = 6.50$) and this result was replicated in the other $GWAS_{SCGG}$ cohort, ($p = 3.78 \times 10^{-10}$, $z = 6.26$) (**Fig. 2** and **Table 1**). Whole blood and lung transcriptome models also identified two additional significant TWAS genes that are specific to one of the two cohorts. Increased expression of *ABO* gene in the lung was associated with risk for the development of severe COVID-19 symptoms in $GWAS_{SCGG}$ data set ($p = 5.98 \times 10^{-7}$, $z = 4.99$). Similarly, increased expression of *GAS7* gene (Growth Arrest-

Specific 7) in whole blood was associated with an increased risk for development of COVID-19 symptom in the $GWAS_{HGI}$ data set ($p = 8.46 \times 10^{-7}$, $z = 4.92$). Overall, these two chemokine receptor genes were found and replicated to be associated with COVID-19 and we used them for further downstream analyses.

Colocalization analysis validated the mediation effect of *CXCR6* between GWAS locus and severe COVID-19

The TWAS findings might be driven by pleiotropy or linkage effect by the LD structure in the GWAS loci instead of the true mediation effect [42] (**Fig. 3a**). To rule out the linkage effect and find further evidence of true colocalization of causal signals in the variants that were significant in both GWAS and eQTL analyses, we performed colocalization analysis by eCAVIAR and fastENLOC using several tissue-specific eQTL datasets. The eCAVIAR with the eQTL data in lung tissue revealed that the severe COVID-19 association could be mediated by the variants that were associated with the expression of *CXCR6* (CLPP = 0.79) (**Table 1**). And the colocalized SNP rs34068335 ($GWAS_{HGI}$ $p = 5.02 \times 10^{-22}$) is also related to the increased monocyte percentage of white cells in a blood-trait GWAS study using Phenoscanner [43-45]. The fastENLOC analysis showed a high RCP between the expression of *CXCR6* in T follicular helper cells and GWAS signal in both the $GWAS_{HGI}$ cohort (RCP=0.99) and the $GWAS_{SCGG}$ cohort (RCP = 0.99) (**Table 1**). However, colocalization analysis of *CCR9* did not suggest strong colocalization evidence (CLPP < 0.1 and RCP < 0.1).

Multi-level functional annotations linked *3p21.31* locus with *CXCR6* and *CCR9* functions

To explore the potential functions linked with the GWAS risk variants, we examined the functional genomic annotations in this locus. Specifically, we found a consistent decreasing effect of *CXCR6* expression in T cells and whole blood from the two large-scaled eQTL datasets (**Fig. 3b**). Furthermore, multiple SNPs at the *3p21.31* locus reside in the annotated regulatory elements across blood, T cell, and lung cell lines (**Fig. 3c,** Methods). The Hi-C cell line data from lung fibroblast [28] also showed a significant interaction between the *3p21.31* locus had interactions with both *CXCR6* and *CCR9* promoter regions (**Fig. 3d**). Overall, these results from the multiple lines of evidence all supported the potential regulatory effects of the *3p21.31* locus on *CXCR6* expression.

CXCR6 differentially expressed in T_{RM} cells of severe and moderate patients

According to our tissue cell-type-specific expression database (CSEA-DB), *CXCR6* is mainly expressed in immune cells in human lung tissue (e.g., T cell and NK cell) [16]. In Liao et al.'s work, the authors reported that *CXCR6* had lower expression in severe patients than moderate patients, indicating a potential protective effect in T cells of human respiratory systems [17]. However, T cells have various resident and circulating subtypes with diverse functions [46]. To understand which subpopulation(s) of T cells might be associated with the severity of COVID-19, we used the BLAF scRNA-seq data of six severe patients and three moderate patients. The data included 6,491 T-cells (4,356 from six severe patients and 2,135 from three moderate patients). We further used a set of 31 T_{RM} cell marker genes to distinguish the T_{RM} cells and conventional $CD8^+$ T cells (Methods). As shown in **Fig. 4a and 4b**, the T_{RM} cells and conventional T cells could be distinguished in both moderate and severe patients with the classic T_{RM} cells markers (*CXCR6* [31], CD69 [47], *ITGAE* (the gene encoding CD103) [47, 48],

ZNF683 [48], and *XCL1* [46]) and three negative-control markers (*SELL* (the gene encoding CD62L) [47], KLF2, and S1PR1 [49]) from previous study [31]. Among the 1,090 lung T_{RM} cells, we found that 675 cells were from moderate patients and only 415 cells were from severe patients. This represented a 3.32-fold decrease for the expected number of T_{RM} cells in severe patients. We used the non-parametric Wilcoxon rank sum test to identify the DEGs in the T_{RM} cells between severe and moderate patients and found *CXCR6* had significantly lower expression in the severe patients than the moderate patients ($p < 2.5 \times 10^{-16}$, fold change = 1.57, **Fig. 4c**).

Inferring the transcriptional programs that drive the cell status transition

To understand the transition between moderate and severe T_{RM} cells, we constructed the cell trajectory/pseudotime along with T_{RM} cells by using Slingshot (**Fig. 4d**) [34]. Next, we applied our DrivAER approach (Driving transcriptional programs based on AutoEncoder derived Relevance scores) [36] to identify the potential transcriptional programs that were most likely involved in the cell trajectory/pseudotime. **Fig. 4e** shows a scaled heatmap to demonstrate the relative expression of naïve and effector markers of T cells in the order of pseudotime generated by Slingshot [34, 39]. We identified that the severe T_{RM} cells were mainly gathered in the later stage of the pseudotime. The naïve markers (*IL7R*, *BCL2*) were higher expressed in moderate patients than in severe patients (except *SELL*). On the contrary, some effector markers (*GZMB, HAVCR2, LAG3, IFNG*) were lower expressed in moderate patients than in severe patients. Other effector markers (*IRF4, PRF1*) had higher expression in the middle of the transition than their expression at the start and end sides. These results indicated that the T_{RM} cells in severe patients still in pro-inflammatory status although the T_{RM} cells status were more heterogeneous in severe patients than in moderate patients (**Fig. 4a, 4b, and 4e**). As shown in **Fig. 4f and 4g**, the top five

molecular signatures (relevance score > 0.25) identified by DrivAER included T-cell pro-inflammatory actions (interferon gamma response, allograft rejection [50], interferon alpha response, and complement system) as well as proliferative mTORC1 signaling pathway [51]. Among the top TFs (relevance score > 0.25) that drove this cell trajectory, the DNA binding RELA-NFKB1 complex is involved in several biological processes, such as inflammation, immunity, and cell growth initiated by external stimuli. The signal transducer and activator of transcription (*STAT1*) and its regulator histone deacetylase (*HDAC1*) could be activated by various ligands including interferon-alpha and interferon-gamma. In summary, the TF results are well consistent with our previous hallmark pathway findings (**Additional file: Table S1 and Table S2**).

Several genome-wide significant SNPs might change the TF binding site affinity

To understand the potential TF binding affinity changes of genome-wide significant SNPs, we conducted the DNA motif recognition analysis of the seven TFs related to the transcriptional program between moderate and severe T_{RM} cells (relevance score > 0.25, **Additional file 1: Table S2**). We identified SNP rs10490770 [T/C, minor allele frequency (MAF) = 0.097, $GWAS_{HGI} = 9.53 \times 10^{-39}$] and SNP rs67959919 (G/A, MAF = 0.097, $GWAS_{HGI} = 8.83 \times 10^{-39}$) that were predicted to alter the binding affinity of TFs RELA and SP1, respectively (**Additional file 1: Fig. S1a and S1b**). Moreover, these two SNPs were in the high LD region ($r^2 > 0.8$) with several significant lead eQTLs (SNP rs35896106 and rs17713054) of *CXCR6* in whole blood ($p = 5.03 \times 10^{-37}$) and T follicular helper cell ($p = 1.30 \times 10^{-5}$) (**Fig. 3b**). In summary, the genome-wide significant SNPs were predicted to change the binding affinity of

322 those TFs highly related to T_{RM} cells status transition, (**Additional file 2: Table S3**), suggesting
323 their potential regulation of *CXCR6* expression.
324
325 **Discussion**
326 In this work, we developed a multi-level, integrative genetic and functional analysis
327 framework to explore the host genetic factors on the expression change of GWAS-implicated
328 genes for COVID-19 severity. Specifically, we conducted TWAS analysis for two independent
329 COVID-19 GWAS datasets. We identified and replicated two chemokine receptor genes, *CXCR6*
330 and *CCR9*, with a protective effect in the lung and a risk effect in whole blood, respectively.
331 *CXCR6* is expressed in T lymphocytes and essential genes in $CD8^+$ T_{RM} cells, mediating the
332 homing of T_{RM} cells to the lung along with its ligand *CXCL16* [52, 53]. *CCR9* was reported to
333 regulate chemotaxis in response to thymus-expressed chemokine in T cells [54]. The
334 colocalization analysis identified that both GWAS and eQTLs of *CXCR6* had high colocalization
335 probabilities in the lung, whole blood, and T follicular helper cells, which confirms the genetic
336 regulation roles at this locus. At the single cell level, our DEG analysis identified *CXCR6* gene
337 had lower expression in the COVID-19 severe patients than the moderate patients in both T cells
338 and T_{RM} cells, supporting its protective effect identified in TWAS analysis in lung and whole
339 blood. The expected proportion of T_{RM} cells also decreased by 3.32-fold (**Table 2**). Interestingly,
340 these findings were replicated in circulating $CXCR6^+$ $CD8^+$ T cells of severe and control/mild
341 patients by flow cytometry experiment [53]. We identified the major transition force from
342 moderate T_{RM} cells to severe T_{RM} cells are pro-inflammatory pathways and TFs.
343 From the TWAS and colocalization analysis in lung and immune cells, we successfully
344 replicated that *CXCR6* was centered in the GWAS signal at locus *3p21.31*. Previous studies have

reported that CXCR6$^{-/-}$ significantly decreases airway lung T_{RM} cells due to altered trafficking of CXCR6$^{-/-}$ cells within the lung of the mice [52], which could explain a much less proportion of T_{RM} cells in severe patients than moderate patients. The lung T_{RM} cells provide the first line of defense against infection and coordinate the subsequent adaptive response [55]. The previous study has reported that T_{RM} cells constitutively expressed surface receptors (PD-1 and CTLA-4) that are associated with inhibition of T cell function, which might prevent excessive activation or inflammation in the tissue niche [56].

We further used nine classic naïve markers (e.g., *BCL2*, *SELL*, *TCF7*, and *IL7R)* and ten classic effector markers (e.g., *GZMB*, *PRF1*, *IFNG*, *LAG3*, and *PDCD1*) to quantify the naïve and effector status of the T_{RM} cells (**Additional file 1: Fig. S2**). T_{RM} cells in severe patients had a much higher median of effector marker score (0.44 in severe and 0.18 in moderate T_{RM} cells) than T_{RM} cells in moderate patients did, suggesting that the severe T_{RM} cells had much higher activities in inflammation as we discovered in **Fig. 4f** despite their proportion decrease. For the naïve score (**Additional file 1: Fig. S2**), both moderate and severe T_{RM} cells had limited expressions (median score: 0.028 in severe and 0.038 in moderate T_{RM} cells). Interestingly, if we removed the lymph node homing receptor *SELL* [31] from the naïve markers list, we would find the median score in severe naïve markers would drop to 0 (**Additional file 1: Fig. S2**). This indicated that *SELL* expression contributed greatly to the naïve status of T_{RM} severe patients. Consistently in **Fig. 4e**, we could also observe that a large proportion of T_{RM} cells had higher *SELL* expression in severe patients than in moderate patients, suggesting the T_{RM} cells in severe patients might not be in a stable cell status due to the lymph node homing signal (*SELL*). To this end, we hypothesized that genetically lower expressed *CXCR6* would decrease the proportion of T_{RM} cells residing in the lung through the CXCR6/CXCL16 axis [52, 53], impairing the first-line

368 defense. Moreover, the lower expression of *CXCR6* would also lead to the "unstable" residency
369 of T_{RM} cells in lung (**Fig. 4b**). The T_{RM} cells play essential roles for orchestrating the immune
370 system, lack of which would lead to severe COVID-19 symptoms, such as acute respiratory
371 distress syndrome, cytokine storm and major multi-organ damage [57] (**Fig. 5**).

372 In this study, we mainly focused on the multi-evidence validated gene *CXCR6* and its
373 mechanism related to severe COVID-19. Although we are unable to directly test the genotype of
374 those severe patients, the association of the single cell level phenotype (lower expression of
375 CXCR6 and decreased proportion of $CD8^+$ $CXCR6^+$ T cells) and the severe COVID-19 has been
376 observed in another work with flow cytometry experiments [53]. We are aware of the genetic
377 factors on *CXCR6* might only explain a proportion of the severe COVID-19 variance. Other
378 genetic mechanisms discovered in GWAS and TWAS analyses need further exploration [6]. The
379 $GWAS_{HGI}$ dataset used in this study was HGI round 4 (alpha), which was the largest GWAS by
380 the access date of October 20, 2020. However, it was not the currently largest GWAS meta-
381 analysis for severe COVID-19 when we prepared the manuscript. This research field is evolving
382 very fast, due to the urgent demand of public health. Currently, the largest GWAS HGI round 4
383 (freeze) contained more samples (4,336 cases/ 353,891 controls), and it included two
384 independent datasets we used in this study. Considering that the $GWAS_{HGI}$ dataset included
385 ~10% control samples from the Asian population, we checked the LocusZoom plot of the chr3:
386 45.80-46.40 million base pairs (Mb) region on GRCh37 reference genome. We found a
387 consistent tendency in GWAS round 4 alpha and freeze version (**Additional file1: Fig. S3**).
388 Another limitation is that the scRNA-seq data only had nine COVID-19 patient samples (six
389 severe and three moderate samples), which might not provide enough statistical power at the
390 sample level as it is commonly considered each scRNA-seq data acts like a population. Finally,

391 the TF binding site affinity alterations were assessed based on computational prediction,
392 therefore, the *in vivo* effects require experimental validation. We anticipate more and larger
393 datasets will be released in the near future. We will apply our integrative analysis approach to
394 such new data.
395
396 **Conclusions**
397 Our work systematically explored the genetic effect on gene expression at chromosome
398 locus *3p21.31* and pinpointed the gene *CXCR6* might be involved in the severity of COVID-19.
399 Several genome-wide significant SNPs were within the LD block of *CXCR6* eQTLs in immune-
400 related cells. In a scRNA-seq COVID-19 BALF dataset, we characterized that *CXCR6* (T_{RM} cells
401 marker gene) had a lower expression in severe patients than in moderate patients. Moreover, the
402 T_{RM} cells in severe patients had a 3.32-fold proportion decrease and much higher pro-
403 inflammatory activity than T_{RM} cells in moderate patients. Based on these observations, we
404 proposed a potential mechanism on how the lower expression of *CXCR6* regulated by the
405 endogenous factors could progress to severe COVID-19 outcomes.
406
407 **List of abbreviations**
408 BALF: bronchoalveolar lavage fluid; BIOS: Biobank-based Integrative Omics Studies;
409 ChromHMM: chromatin-state hidden Markov model; COVID-19: coronavirus disease 2019;
410 CLPP: colocalization posterior probability; CSEA-DB: cell-type-specific expression database;
411 DAP: deterministic approximation of posteriors; DEG: differentially expressed gene; DICE:
412 database of immune cell expression; DrivAER: Driving transcriptional programs based on
413 AutoEncoder derived Relevance scores; eQTL: expression quantitative trait; GReX: genetically

414 regulated expression; GWAS: genome-wide association study; HGI: Host Genetics Initiative; Hi-
415 C: high-throughput chromatin interaction; LD: linkage disequilibrium; MAF: minor allele
416 frequency; MASHR: multivariate adaptive shrinkage in R; Mb: million base pairs; MSigDB:
417 molecular signatures database; PIP: posterior inclusion probability; PWM: position weight
418 matrix; SARS-CoV-2: severe acute respiratory syndrome coronavirus 2; RCP: regional
419 colocalization probability; SCGG: Severe COVID-19 GWAS Group; scRNA-seq: single cell
420 RNA sequencing; tSNE: t-Distributed Stochastic Neighbor Embedding; TF: transcription factor;
421 T_{RM} cells: resident memory CD8+ T cells; TWAS: transcriptome-wide association study;
422

423 **Funding**

424 Dr. Zhao was partially supported by National Institutes of Health grant R01LM012806 and Chair
425 Professorship for Precision Health funds. We thank the technical support from the Cancer
426 Genomics Core funded by the Cancer Prevention and Research Institute of Texas (CPRIT
427 RP180734). The funders had no role in the study design, data collection and analysis, decision to
428 publish, or preparation of the manuscript.

429 **Acknowledgements**

430 We appreciate Drs. Teng Liu and Dawei Zou for the valuable comments. We thank all members
431 of the Bioinformatics and Systems Medicine Laboratory for the discussion.

432
433

References

1. Zhao Z, Li H, Wu X, Zhong Y, Zhang K, Zhang YP, Boerwinkle E, Fu YX: **Moderate mutation rate in the SARS coronavirus genome and its implications.** *BMC Evol Biol* 2004, **4:**21.
2. Liu S, Shen J, Fang S, Li K, Liu J, Yang L, Hu CD, Wan J: **Genetic Spectrum and Distinct Evolution Patterns of SARS-CoV-2.** *Front Microbiol* 2020, **11:**593548.
3. Wu Z, McGoogan JM: **Characteristics of and Important Lessons From the Coronavirus Disease 2019 (COVID-19) Outbreak in China: Summary of a Report of 72314 Cases From the Chinese Center for Disease Control and Prevention.** *JAMA* 2020, **323:**1239-1242.
4. Bhopal SS, Bhopal R: **Sex differential in COVID-19 mortality varies markedly by age.** vol. 396. pp. 532-533: Lancet Publishing Group; 2020:532-533.
5. Severe Covid GG, Ellinghaus D, Degenhardt F, Bujanda L, Buti M, Albillos A, Invernizzi P, Fernandez J, Prati D, Baselli G, et al: **Genomewide Association Study of Severe Covid-19 with Respiratory Failure.** *N Engl J Med* 2020, **383:**1522-1534.
6. Pairo-Castineira E, Clohisey S, Klaric L, Bretherick AD, Rawlik K, Pasko D, Walker S, Parkinson N, Fourman MH, Russell CD, et al: **Genetic mechanisms of critical illness in Covid-19.** *Nature* 2020.
7. GTEx Consortium: **The GTEx Consortium atlas of genetic regulatory effects across human tissues.** *Science* 2020, **369:**1318-1330.
8. Võsa U, Claringbould A, Westra H-J, Bonder MJ, Deelen P, Zeng B, Kirsten H, Saha A, Kreuzhuber R, Kasela S, et al: **Unraveling the polygenic architecture of complex traits using blood eQTL metaanalysis.** *bioRxiv* 2018**:**447367.
9. Schmiedel BJ, Singh D, Madrigal A, Valdovino-Gonzalez AG, White BM, Zapardiel-Gonzalo J, Ha B, Altay G, Greenbaum JA, McVicker G, et al: **Impact of Genetic Polymorphisms on Human Immune Cell Gene Expression.** *Cell* 2018, **175:**1701-1715 e1716.
10. Gamazon ER, Wheeler HE, Shah KP, Mozaffari SV, Aquino-Michaels K, Carroll RJ, Eyler AE, Denny JC, Consortium GT, Nicolae DL, et al: **A gene-based association method for mapping traits using reference transcriptome data.** *Nat Genet* 2015, **47:**1091-1098.
11. Giambartolomei C, Vukcevic D, Schadt EE, Franke L, Hingorani AD, Wallace C, Plagnol V: **Bayesian test for colocalisation between pairs of genetic association studies using summary statistics.** *PLoS Genet* 2014, **10:**e1004383.
12. Dai Y, Pei G, Zhao Z, Jia P: **A Convergent Study of Genetic Variants Associated With Crohn's Disease: Evidence From GWAS, Gene Expression, Methylation, eQTL and TWAS.** *Front Genet* 2019, **10:**318.
13. Dai Y, Hu R, Pei G, Zhang H, Zhao Z, Jia P: **Diverse types of genomic evidence converge on alcohol use disorder risk genes.** *J Med Genet* 2020, **57:**733-743.
14. Mathys H, Davila-Velderrain J, Peng Z, Gao F, Mohammadi S, Young JZ, Menon M, He L, Abdurrob F, Jiang X, et al: **Single-cell transcriptomic analysis of Alzheimer's disease.** *Nature* 2019, **570:**332-337.
15. Papalexi E, Satija R: **Single-cell RNA sequencing to explore immune cell heterogeneity.** *Nat Rev Immunol* 2018, **18:**35-45.

16. Dai Y, Hu R, Manuel AM, Liu A, Jia P, Zhao Z: **CSEA-DB: an omnibus for human complex trait and cell type associations.** *Nucleic Acids Res* 2021, **49:**D862-D870.
17. Liao M, Liu Y, Yuan J, Wen Y, Xu G, Zhao J, Cheng L, Li J, Wang X, Wang F, et al: **Single-cell landscape of bronchoalveolar immune cells in patients with COVID-19.** *Nat Med* 2020, **26:**842-844.
18. Barbeira AN, Dickinson SP, Bonazzola R, Zheng J, Wheeler HE, Torres JM, Torstenson ES, Shah KP, Garcia T, Edwards TL, et al: **Exploring the phenotypic consequences of tissue specific gene expression variation inferred from GWAS summary statistics.** *Nature Communications* 2018, **9:**1-20.
19. Urbut SM, Wang G, Carbonetto P, Stephens M: **Flexible statistical methods for estimating and testing effects in genomic studies with multiple conditions.** *Nat Genet* 2019, **51:**187-195.
20. Hormozdiari F, van de Bunt M, Segrè AV, Li X, Joo JWJ, Bilow M, Sul JH, Sankararaman S, Pasaniuc B, Eskin E: **Colocalization of GWAS and eQTL Signals Detects Target Genes.** *American Journal of Human Genetics* 2016, **99:**1245-1260.
21. Wen X, Pique-Regi R, Luca F: **Integrating molecular QTL data into genome-wide genetic association analysis: Probabilistic assessment of enrichment and colocalization.** *PLOS Genetics* 2017, **13:**e1006646-e1006646.
22. Genomes Project C, Auton A, Brooks LD, Durbin RM, Garrison EP, Kang HM, Korbel JO, Marchini JL, McCarthy S, McVean GA, Abecasis GR: **A global reference for human genetic variation.** *Nature* 2015, **526:**68-74.
23. Lee Y, Luca F, Pique-Regi R, Wen X: **Bayesian Multi-SNP genetic association analysis: Control of FDR and use of summary statistics.** pp. 316471-316471: bioRxiv; 2018:316471-316471.
24. Võsa U, Claringbould A, Westra HJ, Bonder MJ, Deelen P, Zeng B, Kirsten H, Saha A, Kreuzhuber R, Kasela S, et al: **Unraveling the polygenic architecture of complex traits using blood eQTL meta-analysis.** vol. 18. pp. 10-10: bioRxiv; 2018:10-10.
25. Zhernakova DV, Deelen P, Vermaat M, van Iterson M, van Galen M, Arindrarto W, van 't Hof P, Mei H, van Dijk F, Westra HJ, et al: **Identification of context-dependent expression quantitative trait loci in whole blood.** *Nat Genet* 2017, **49:**139-145.
26. Ernst J, Kellis M: **ChromHMM: automating chromatin-state discovery and characterization.** *Nat Methods* 2012, **9:**215-216.
27. Roadmap Epigenomics C, Kundaje A, Meuleman W, Ernst J, Bilenky M, Yen A, Heravi-Moussavi A, Kheradpour P, Zhang Z, Wang J, et al: **Integrative analysis of 111 reference human epigenomes.** *Nature* 2015, **518:**317-329.
28. Dixon JR, Selvaraj S, Yue F, Kim A, Li Y, Shen Y, Hu M, Liu JS, Ren B: **Topological domains in mammalian genomes identified by analysis of chromatin interactions.** *Nature* 2012, **485:**376-380.
29. Hahne F, Ivanek R: **Visualizing genomic data using Gviz and bioconductor.** In *Volume* 1418: Humana Press Inc.; 2016: 335-351
30. Liu T, Jia P, Fang B, Zhao Z: **Differential Expression of Viral Transcripts From Single-Cell RNA Sequencing of Moderate and Severe COVID-19 Patients and Its Implications for Case Severity.** *Front Microbiol* 2020, **11:**603509.

31. Kumar BV, Ma W, Miron M, Granot T, Guyer RS, Carpenter DJ, Senda T, Sun X, Ho SH, Lerner H, et al: **Human Tissue-Resident Memory T Cells Are Defined by Core Transcriptional and Functional Signatures in Lymphoid and Mucosal Sites.** *Cell Rep* 2017, **20:**2921-2934.
32. Pont F, Tosolini M, Fournie JJ: **Single-Cell Signature Explorer for comprehensive visualization of single cell signatures across scRNA-seq datasets.** *Nucleic Acids Res* 2019, **47:**e133.
33. Stuart T, Butler A, Hoffman P, Hafemeister C, Papalexi E, Mauck WM, 3rd, Hao Y, Stoeckius M, Smibert P, Satija R: **Comprehensive Integration of Single-Cell Data.** *Cell* 2019, **177:**1888-1902 e1821.
34. Street K, Risso D, Fletcher RB, Das D, Ngai J, Yosef N, Purdom E, Dudoit S: **Slingshot: cell lineage and pseudotime inference for single-cell transcriptomics.** *BMC Genomics* 2018, **19:**477.
35. Hastie T, Stuetzle W: **Principal Curves.** *Journal of the American Statistical Association* 1989, **84:**502-516.
36. Simon LM, Yan F, Zhao Z: **DrivAER: Identification of driving transcriptional programs in single-cell RNA sequencing data.** *Gigascience* 2020, **9**.
37. Eraslan G, Simon LM, Mircea M, Mueller NS, Theis FJ: **Single-cell RNA-seq denoising using a deep count autoencoder.** *Nat Commun* 2019, **10:**390.
38. Liberzon A, Birger C, Thorvaldsdottir H, Ghandi M, Mesirov JP, Tamayo P: **The Molecular Signatures Database (MSigDB) hallmark gene set collection.** *Cell Syst* 2015, **1:**417-425.
39. Han H, Cho JW, Lee S, Yun A, Kim H, Bae D, Yang S, Kim CY, Lee M, Kim E, et al: **TRRUST v2: an expanded reference database of human and mouse transcriptional regulatory interactions.** *Nucleic Acids Res* 2018, **46:**D380-D386.
40. Nguyen NTT, Contreras-Moreira B, Castro-Mondragon JA, Santana-Garcia W, Ossio R, Robles-Espinoza CD, Bahin M, Collombet S, Vincens P, Thieffry D, et al: **RSAT 2018: regulatory sequence analysis tools 20th anniversary.** *Nucleic Acids Res* 2018, **46:**W209-W214.
41. Weirauch MT, Yang A, Albu M, Cote AG, Montenegro-Montero A, Drewe P, Najafabadi HS, Lambert SA, Mann I, Cook K, et al: **Determination and inference of eukaryotic transcription factor sequence specificity.** *Cell* 2014, **158:**1431-1443.
42. Wainberg M, Sinnott-Armstrong N, Mancuso N, Barbeira AN, Knowles DA, Golan D, Ermel R, Ruusalepp A, Quertermous T, Hao K, et al: **Opportunities and challenges for transcriptome-wide association studies.** *Nat Genet* 2019, **51:**592-599.
43. Astle WJ, Elding H, Jiang T, Allen D, Ruklisa D, Mann AL, Mead D, Bouman H, Riveros-Mckay F, Kostadima MA, et al: **The Allelic Landscape of Human Blood Cell Trait Variation and Links to Common Complex Disease.** *Cell* 2016, **167:**1415-1429.e1419.
44. Kamat MA, Blackshaw JA, Young R, Surendran P, Burgess S, Danesh J, Butterworth AS, Staley JR: **PhenoScanner V2: An expanded tool for searching human genotype-phenotype associations.** *Bioinformatics* 2019, **35:**4851-4853.
45. Staley JR, Blackshaw J, Kamat MA, Ellis S, Surendran P, Sun BB, Paul DS, Freitag D, Burgess S, Danesh J, et al: **PhenoScanner: A database of human genotype-phenotype associations.** *Bioinformatics* 2016, **32:**3207-3209.

46. Hombrink P, Helbig C, Backer RA, Piet B, Oja AE, Stark R, Brasser G, Jongejan A, Jonkers RE, Nota B, et al: **Programs for the persistence, vigilance and control of human CD8(+) lung-resident memory T cells.** *Nat Immunol* 2016, **17:**1467-1478.
47. Martin MD, Badovinac VP: **Defining Memory CD8 T Cell.** *Front Immunol* 2018, **9:**2692.
48. Wauters E, Van Mol P, Garg AD, Jansen S, Van Herck Y, Vanderbeke L, Bassez A, Boeckx B, Malengier-Devlies B, Timmerman A, et al: **Discriminating mild from critical COVID-19 by innate and adaptive immune single-cell profiling of bronchoalveolar lavages.** *Cell Res* 2021.
49. Skon CN, Lee JY, Anderson KG, Masopust D, Hogquist KA, Jameson SC: **Transcriptional downregulation of S1pr1 is required for the establishment of resident memory CD8+ T cells.** *Nat Immunol* 2013, **14:**1285-1293.
50. Benichou G, Gonzalez B, Marino J, Ayasoufi K, Valujskikh A: **Role of Memory T Cells in Allograft Rejection and Tolerance.** *Front Immunol* 2017, **8:**170.
51. Yu JS, Cui W: **Proliferation, survival and metabolism: the role of PI3K/AKT/mTOR signalling in pluripotency and cell fate determination.** *Development* 2016, **143:**3050-3060.
52. Wein AN, McMaster SR, Takamura S, Dunbar PR, Cartwright EK, Hayward SL, McManus DT, Shimaoka T, Ueha S, Tsukui T, et al: **CXCR6 regulates localization of tissue-resident memory CD8 T cells to the airways.** *J Exp Med* 2019, **216:**2748-2762.
53. Payne DJ, Dalal S, Leach R, Parker R, Griffin S, McKimmie CS, Cook GP, Richards SJ, Hillmen P, Munir T, et al: **The CXCR6/CXCL16 axis links inflamm-aging to disease severity in COVID-19 patients.** *bioRxiv* 2021**:**2021.2001.2025.428125.
54. Lee HS, Kim HR, Lee EH, Jang MH, Kim SB, Park JW, Seoh JY, Jung YJ: **Characterization of CCR9 expression and thymus-expressed chemokine responsiveness of the murine thymus, spleen and mesenteric lymph node.** *Immunobiology* 2012, **217:**402-411.
55. Ardain A, Marakalala MJ, Leslie A: **Tissue-resident innate immunity in the lung.** *Immunology* 2020, **159:**245-256.
56. Szabo PA, Miron M, Farber DL: **Location, location, location: Tissue resident memory T cells in mice and humans.** *Sci Immunol* 2019, **4**.
57. Tay MZ, Poh CM, Renia L, MacAry PA, Ng LFP: **The trinity of COVID-19: immunity, inflammation and intervention.** *Nat Rev Immunol* 2020, **20:**363-374.

599 **Figure legends**

600 **Fig. 1** Workflow of a data-driven study: from genetic factor to molecular phenotype.

601 The study has four major levels. Level 1: we collected the current largest COVID-19 genome-
602 wide association study (GWAS) datasets and a non-duplicated replicate of the severe COVID-19
603 GWAS dataset. Level 2: we utilized the cutting-edge statistical approaches (transcriptome-wide
604 association study and colocalization analysis) and public functional genomics annotations to
605 dissect the genetic effects on gene expression (Methods). Then, we cross-validated our findings
606 of these methods to ensure the robustness. Level 3: we adapted single cell RNA sequencing
607 dataset from COVID-19 bronchoalveolar lavage fluid samples. We applied differentially
608 expressed gene analysis and machine learning methods to characterize the molecular changes of
609 candidate gene at single cell level from COVID-19 moderate and severe patients. We conducted
610 extensive literature review to explain our observations. Level 4: we proposed a mechanism for
611 explaining the "causal" association of genetic factors and the severity of COVID-19 patients.

612

613 **Fig. 2** Manhattan plots illustrating the z scores of transcriptome-wide association study (TWAS)
614 genes.

615 TWAS z scores for two genome-wide association study (GWAS) datasets of susceptibility to
616 severe COVID-19 using lung and whole blood tissue models. The upper panel shows the results
617 from $GWAS_{HGI}$ and the lower panel from $GWAS_{SCGG}$ (see Methods). The round and triangle
618 points denote lung and whole blood tissues, respectively, in the TWAS analysis. Dashed
619 horizontal lines denote the Bonferroni-corrected significance threshold ($|z| = 4.56$, $p < 5 \times 10^{-6}$).
620 Significant genes were highlighted with their gene symbol.

621

Fig. 3 Functional genomic annotation on *3p21.31* locus with signals from $GWAS_{HGI}$.

(**a**) LocusZoom view of the association signals of SNPs at the *3p21.31* locus of $GWAS_{HGI}$. The x-axis is the chromosome position in million base pairs (Mb) on GRCh37 reference genome and y-axis represents the $-\log_{10}$ (p-value) from $GWAS_{HGI}$ dataset. The color indicates the strength of linkage disequilibrium from the lead SNP rs35081325. The genes within the region are annotated in the lower panel. A vertical blue line labels the position of the lead SNP rs35081325 to denote the relationship of GWAS variants to other datasets: expression quantitative trait (eQTL) (Fig. 3b), chromatin interaction (Fig. 3c), and imputed Roadmap functional elements (Fig. 3d). (**b**) The significant eQTLs associated with *CXCR6* expression in this region. The *cis*- eQTL datasets include two whole blood datasets [Biobank-based Integrative Omics Studies (BIOS) QTL and eQTLGen] and one T follicular helper cell dataset (DICE). The y axis represents the $-\log_{10}$ (p-value) from the eQTL studies. (**c**) The significant Hi-C interactions in normal lung fibroblast cell line (IMR90). Blue blocks denote the target and bait regions, and red arcs indicate the interactions between functional elements. (**d**) The region annotated with the chromatin-state segmentation track (ChromHMM) from the Roadmap Epigenomics data for T-cell and lung tissue. The Roadmap Epigenomics cell line IDs are shown on the left side: E017 (IMR90 fetal lung fibroblasts Cell Line), E033 (Primary T Cells from cord blood), E034 (Primary T Cells from blood), E038 (Primary T help naïve cells from peripheral blood), E039 (Primary T helper naïve cells from peripheral blood), E040 (Primary T helper memory cells from peripheral blood 1), E041 (Primary T helper cells PMA-Ionomycin stimulated), E042 (Primary T helper 17 cells PMA-Ionomycin stimulated), E043 (Primary T helper cells from peripheral blood), E044 (Primary T regulatory cells from peripheral blood), E045 (Primary T cells effector/memory enriched from peripheral blood), E047 (Primary T CD8 naïve cells from peripheral blood), E048

(Primary T CD8 memory cells from peripheral blood), E088 (Fetal lung), E096 (Lung), E114 (A549 EtOH 0.02pct Lung Carcinoma Cell Line), and E128 (NHLF Human Lung Fibroblast Primary Cells). The colors denote chromatin states imputed by ChromHMM, with the color key in the gray box (Methods).

Fig. 4 Single cell transcriptome analysis of the severe and moderate COVID-19 patients. (**a**) Relative expression of the lung resident memory $CD8^+$ T (T_{RM}) signature genes in T_{RM} cells and conventional $CD8^+$ T cells in moderate patients. (**b**) Relative expression of the T_{RM} featured genes in T_{RM} cells and conventional $CD8^+$ T cells in severe patients. (**c**) *CXCR6* expression in the T_{RM} cells of moderate and severe patients. We split the T_{RM} cells from the annotation of the original paper with 31 marker genes (Methods). We conducted a two-sided non-parameter Wilcoxon rank sum test to test whether *CXCR6* was differentially expressed in moderate (red) and severe (blue) groups of T_{RM} cells. "***" indicates it is genome-wide significant after multiple-test correction of all expressed genes. The small points denote the normalized expression in each cell. Mean normalized expression of *CXCR6* in each group is highlighted with the largest circle in black. (**d**) Pseudotime inference for the moderate and severe T_{RM} cells. The red and blue points on t-Distributed Stochastic Neighbor Embedding (tSNE) projection denote the T_{RM} cells from moderate and severe patients, respectively. The x-axis and y-axis are the first and second dimension of the tSNE, respectively. (**e**) Relative expression of the *CXCR6* and naïve and effector T cell markers along the pseudotime proportional to the green color. The gene expressions are scaled by cells. Cells from moderate and severe groups are annotated in blue and red. (**f**) Relevance score for hallmark pathways from the molecular signatures database (MSigDB) along the pseudotime. The relevance score (R^2 coefficient of determination) indicates

668 the proportion of variance in the pseudotime explained by the genes in the hallmark pathways.
669 (**g**) Relevance score for transcription factors and their target genes along the pseudotime. The
670 relevance score denotes the proportion of variance in the pseudotime explained by the target
671 genes regulated by the transcription factor.
672
673 **Fig. 5** The proposed *CXCR6* regulation mechanism on COVID-19 severity.
674 We proposed one pathogenesis mechanism using current knowledge to explain how the lower
675 expression of *CXCR6* could be associated with the outcome of severe COVID-19 symptoms,
676 which was supported by our findings of the genetic factors on decreasing the *CXCR6* expression
677 and aligned with our observations from single cell transcriptome analysis. The star on the DNA
678 indicates the host genetic effects.
679

680 **Table 1:** Summary of TWAS and colocalization analyses in tissues and cell lines.

Gene symbol	Tissue	Discovery: $GWAS_{HGI}$				Validation: $GWAS_{SCGG}$			
		TWAS z	TWAS p	PP	colocalized SNP p	TWAS z	TWAS p	PP	colocalized SNP p
CXCR6	Lung	-8.53	1.57×10^{-17}	0.79*	rs34068335 5.02×10^{-22}	-4.19	2.84×10^{-5}	ns	-
	T follicular helper cells	-	-	0.99**	rs35081325 3.82×10^{-39}	-	-	0.99**	rs35081325 2.49×10^{-10}
CCR9	Whole blood	6.50	7.90×10^{-11}	ns	-	6.26	3.78×10^{-10}	ns	-

681 $GWAS_{HGI}$ denotes the GWAS dataset from the Host Genetics Initiative.

682 $GWAS_{SCGG}$ represents the GWAS dataset from the Severe COVID-19 GWAS Group.

683 PP: posterior probability.

684 z: z score.

685 p: p-value.

686 *: statistically significant by the colocalization posterior probability (CLPP) from eCAVIAR.

687 **: statistically significant by the regional colocalization probability (RCP) from fastENLOC.

688 ns: no significant colocalization from either eCAVIAR or fastENLOC.

689 -: no available data.
690

691 **Table 2:** Counts and ratio of T_{RM} cells in moderate and severe patients.

Patient group (sample size)	# $CD8^+$ T cells	# T_{RM} cells	T_{RM} cell proportion ratio (Moderate/Severe)
Moderate (3)	2,135	675	3.32
Severe (6)	4,356	415	

692 #: the counted number.

693 T_{RM} cells: the resident memory $CD8^+$ T cells as defined in Methods.
694

695

Additional files

Additional file 1.pdf: Fig S1: Sequence logos representing DNA binding site generated from position weight matrix (PWM) for transcription factor RELA and SP1. Fig. S2. Violin plots showing the distribution of key features between moderate and severe patients. Fig. S3. LocusZoom views for two Host Genetics Initiates GWAS datasets at *3p21.31* locus. Table S1: Hallmark pathways and their relevance scores. Table S2: Transcription factors and their relevance scores.

Additional file 2.xls: Table S3: Predicted transcription factors (SP1 and RELA) bind affinity alterations on genome-wide significant SNPs at locus *3p21.31*.

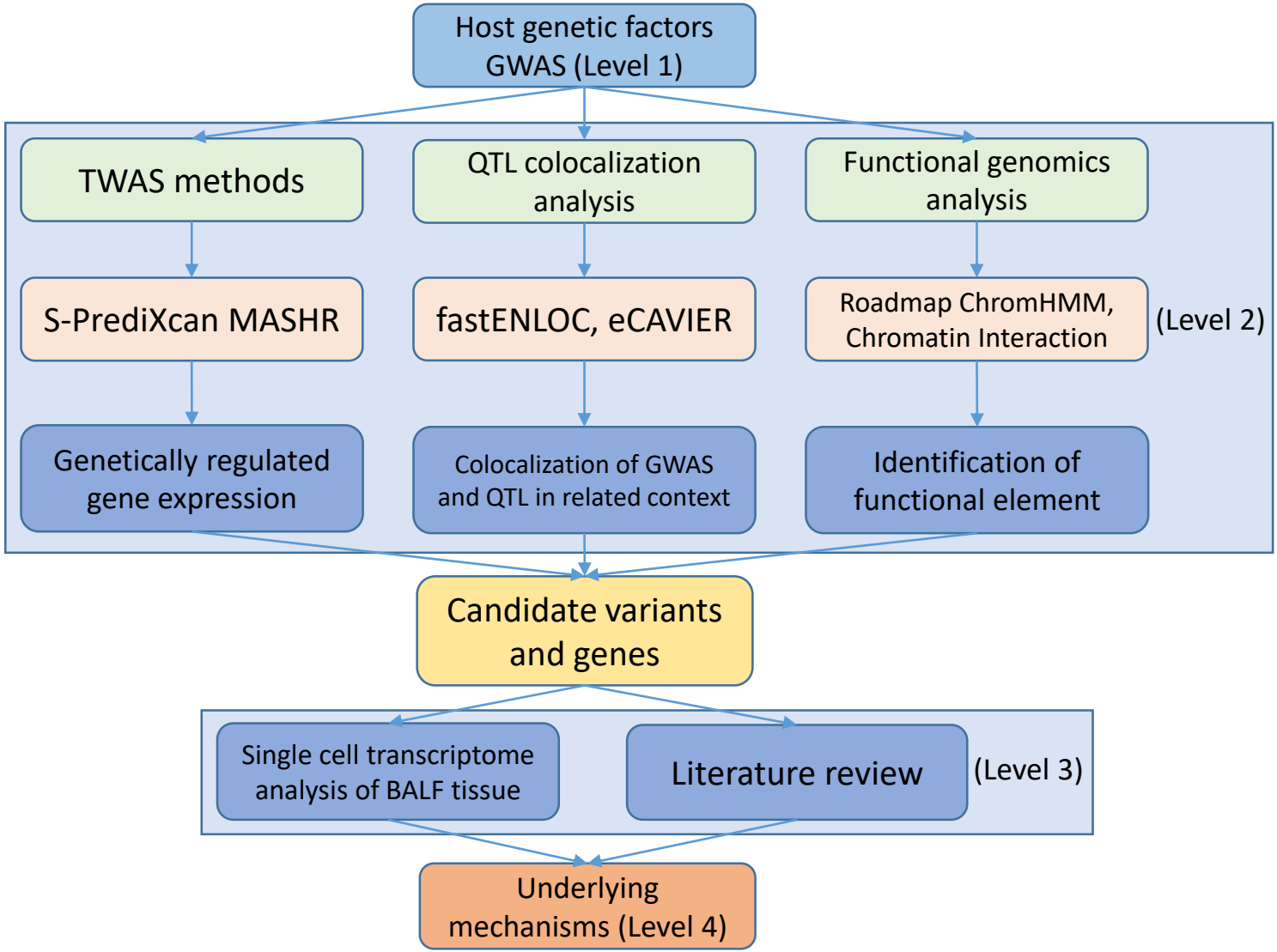
Host genetic factors GWAS (Level 1)
TWAS methods
QTL colocalization analysis
Functional genomics analysis
S-PrediXcan MASHR
fastENLOC, eCAVIER
Roadmap ChromHMM, Chromatin Interaction
(Level 2)
Genetically regulated gene expression
Colocalization of GWAS and QTL in related context
Identification of functional element
Candidate variants and genes
Single cell transcriptome analysis of BALF tissue
Literature review
(Level 3)
Underlying mechanisms (Level 4)

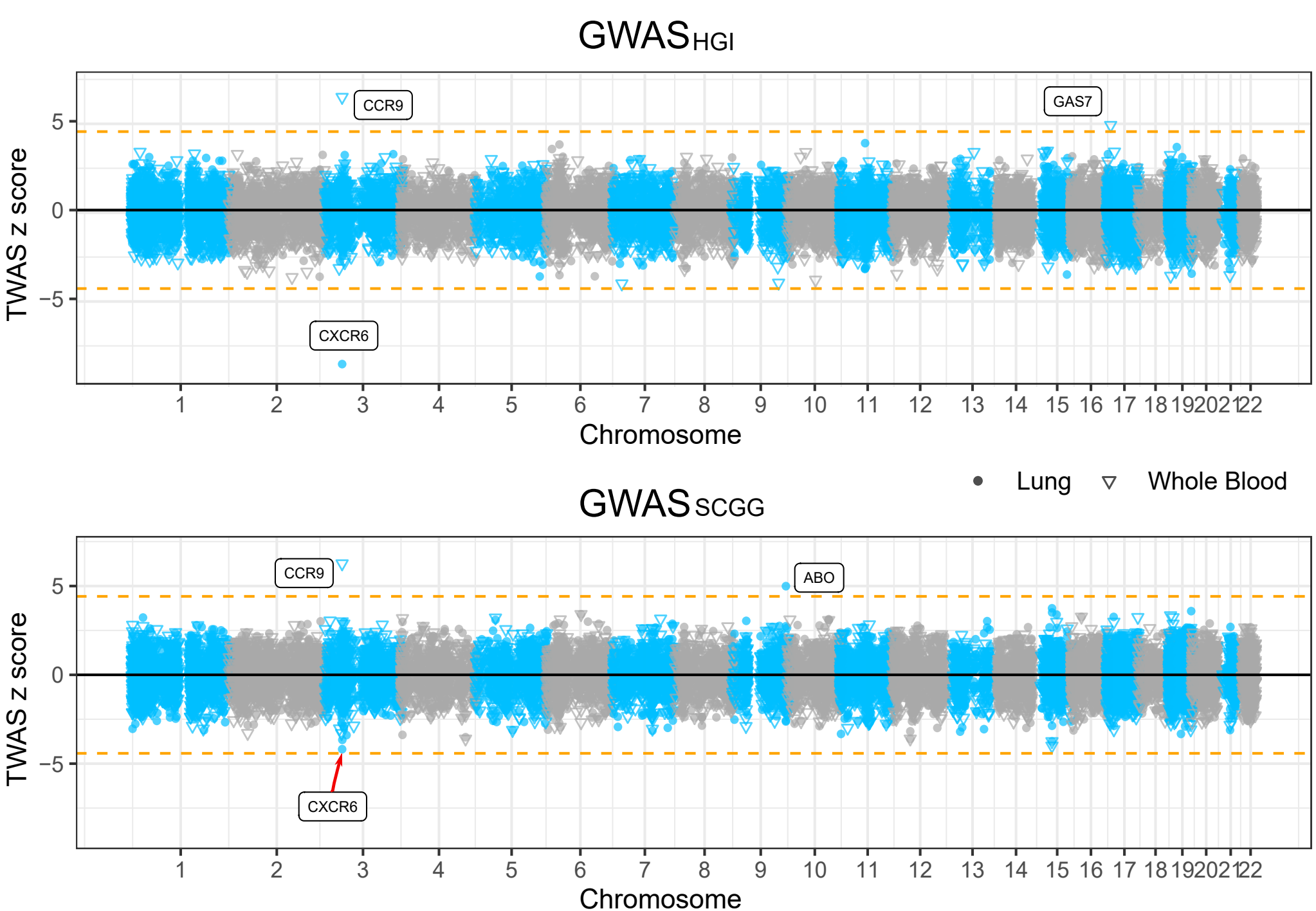
GWAS HGI
CCR9
GAS7
CXCR6
TWAS z score
5
0
−5
1
2
3
4
5
6
7
8
9
10
11
12
13
14
15
16
17
18
19
20
21
22
Chromosome
Lung
Whole Blood
GWAS SCGG
CCR9
ABO
CXCR6
TWAS z score
Chromosome

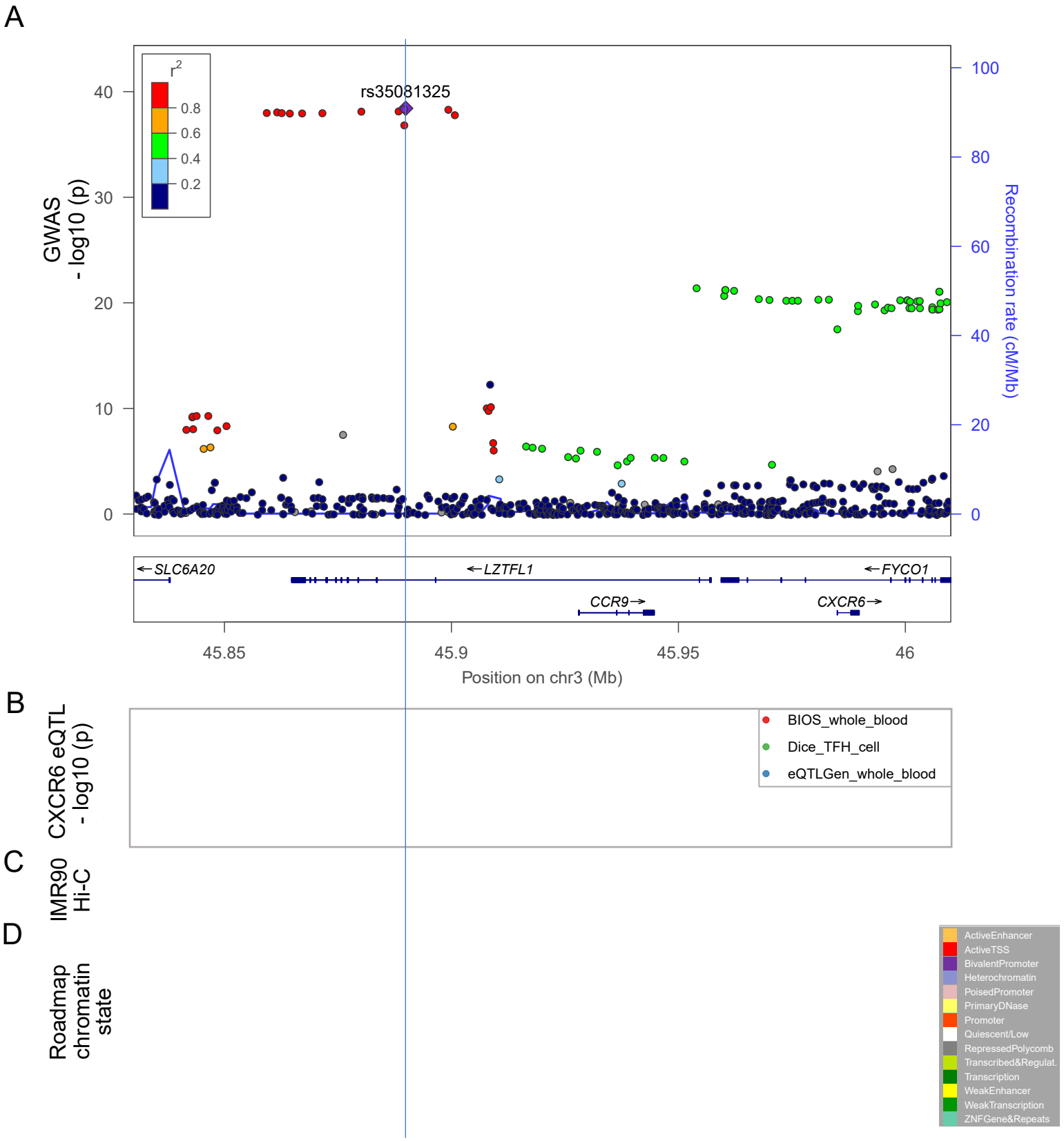
A
r2
0.8
0.6
0.4
0.2
rs35081325
GWAS
- log10 (p)
Recombination rate (cM/Mb)
SLC6A20
LZTFL1
FYCO1
CCR9
CXCR6
45.85
45.9
45.95
46
Position on chr3 (Mb)
B
CXCR6 eQTL
- log10 (p)
BIOS_whole_blood
Dice_TFH_cell
eQTLGen_whole_blood
C
IMR90
Hi-C
D
Roadmap
chromatin
state
ActiveEnhancer
ActiveTSS
BivalentPromoter
Heterochromatin
PoisedPromoter
PrimaryDNase
Promoter
Quiescent/Low
RepressedPolycomb
Transcribed&Regulat.
Transcription
WeakEnhancer
WeakTranscription
ZNFGene&Repeats

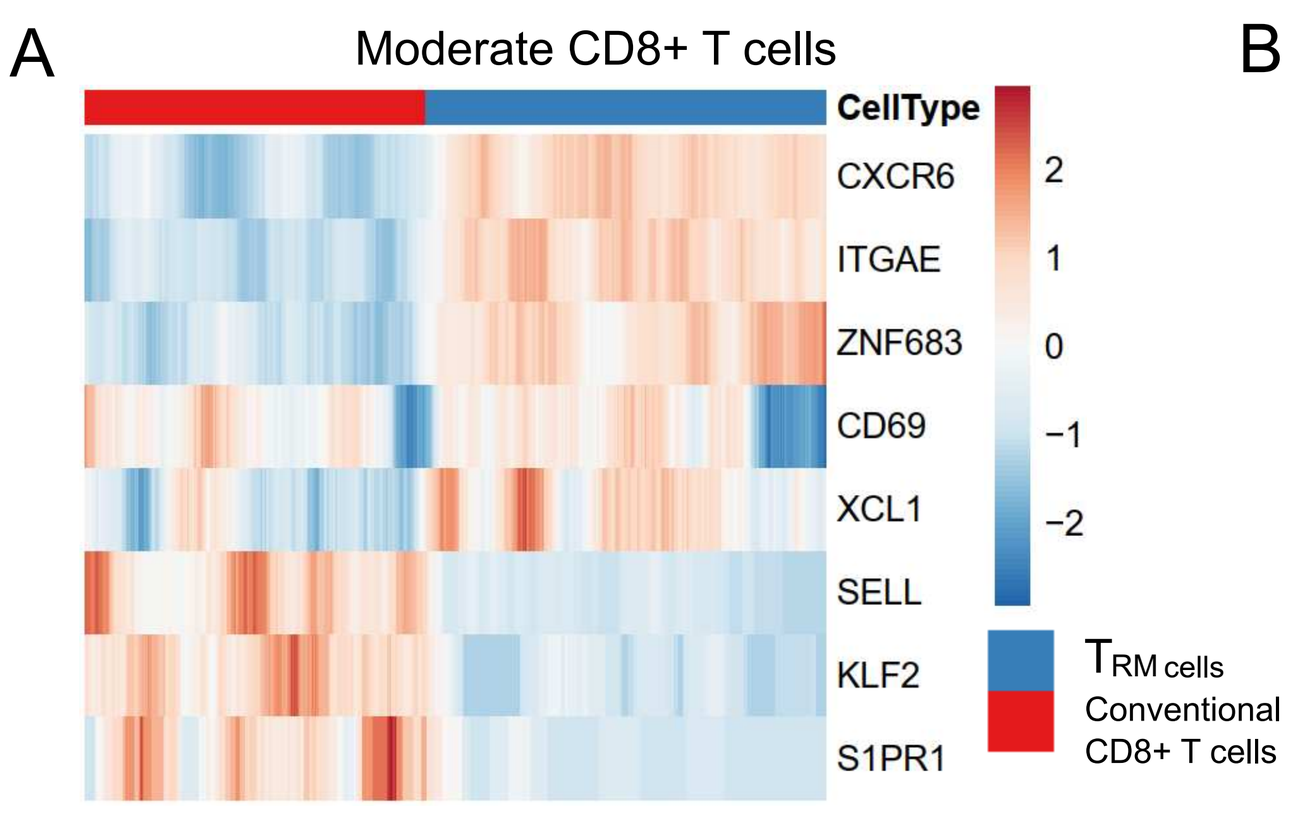

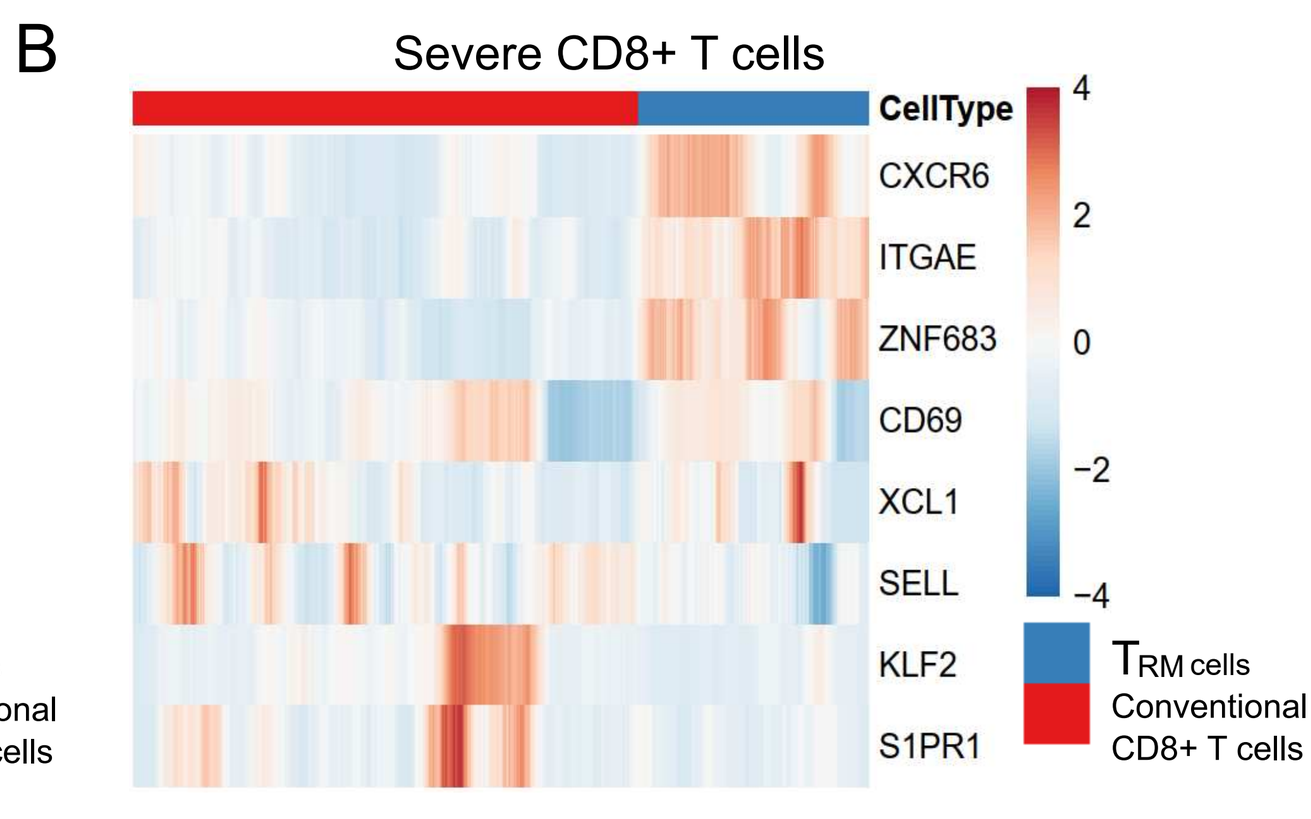

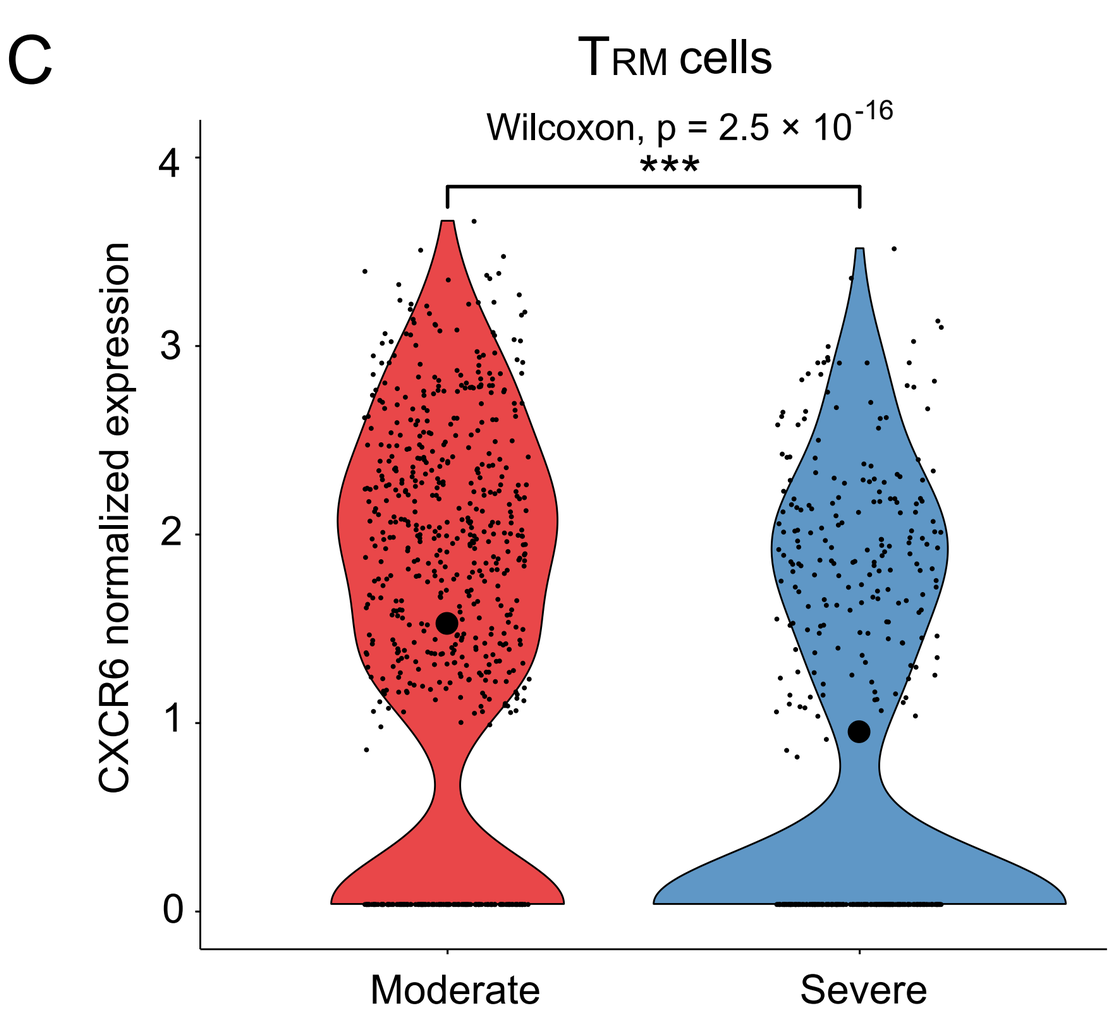

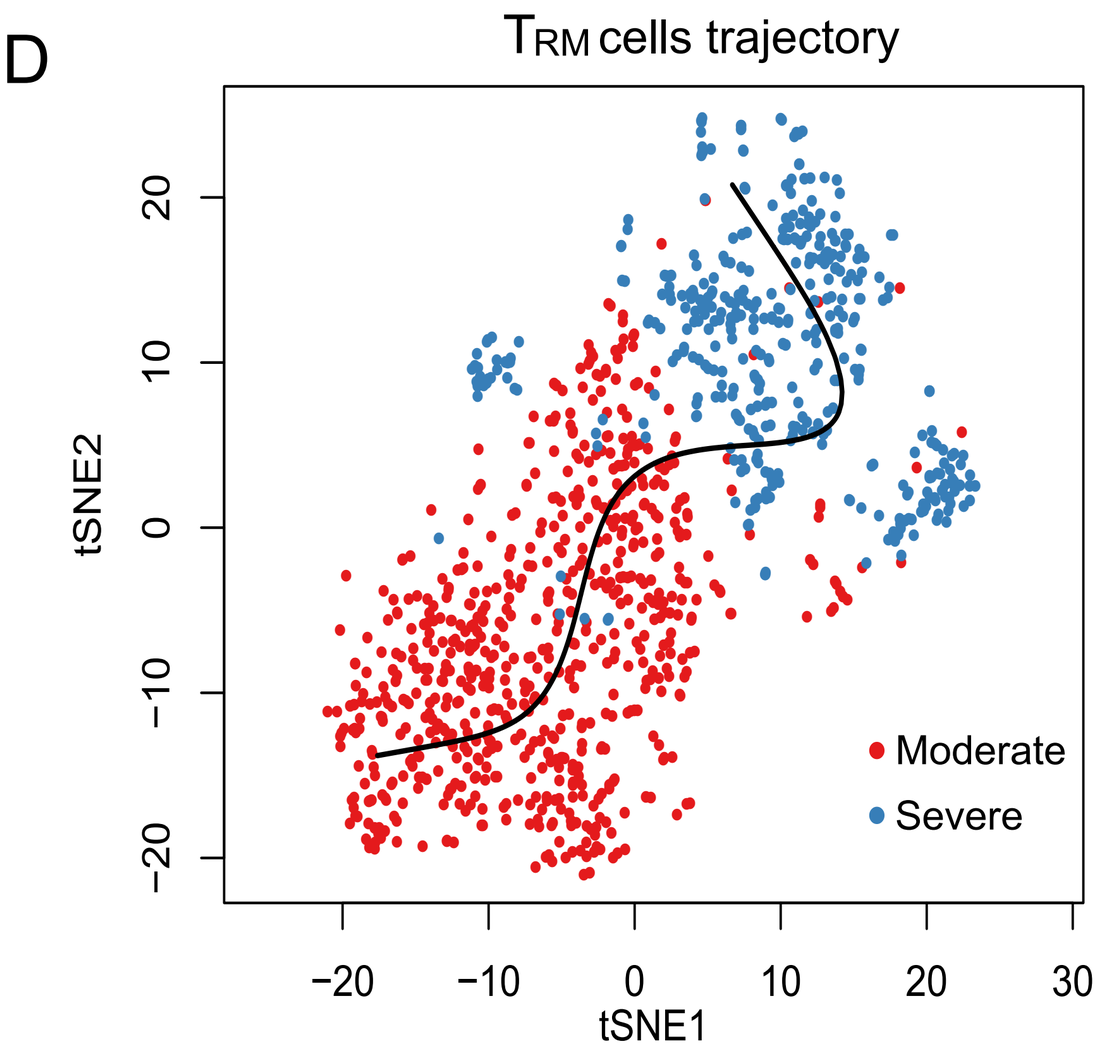

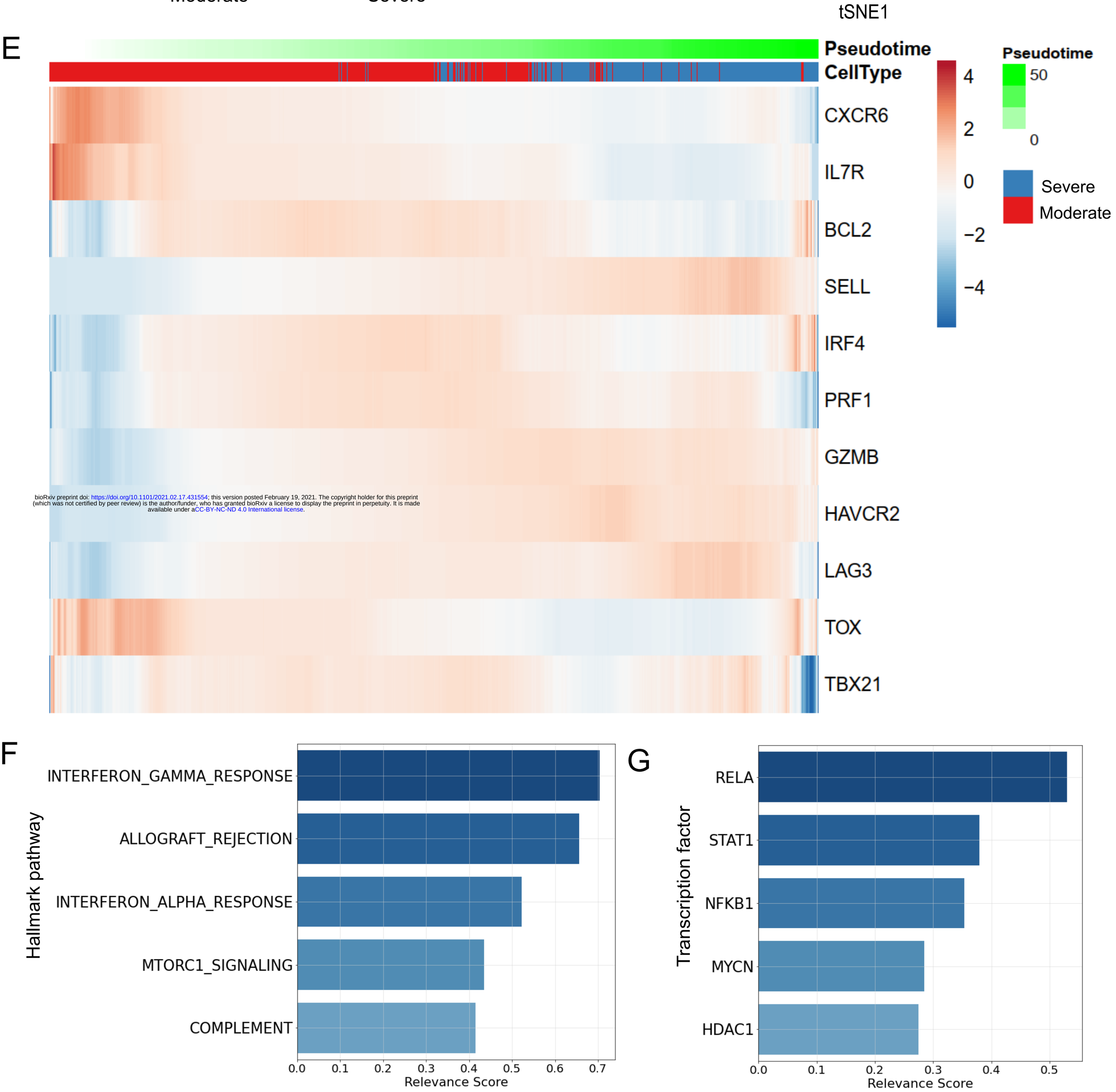

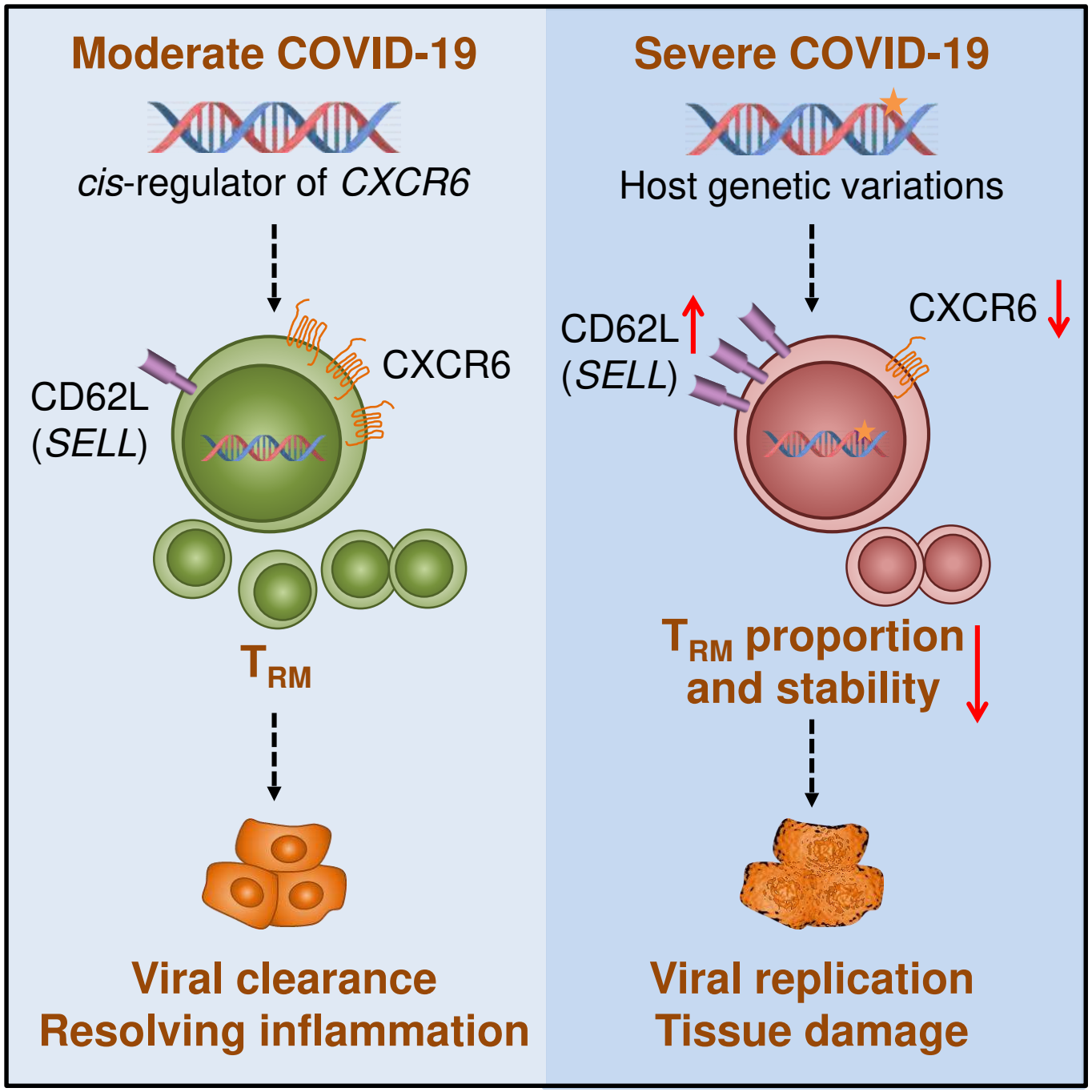
Moderate COVID-19
cis-regulator of CXCR6
CD62L
(SELL)
CXCR6
TRM
Viral clearance
Resolving inflammation
Severe COVID-19
Host genetic variations
CD62L
(SELL)
CXCR6
TRM proportion
and stability
Viral replication
Tissue damage